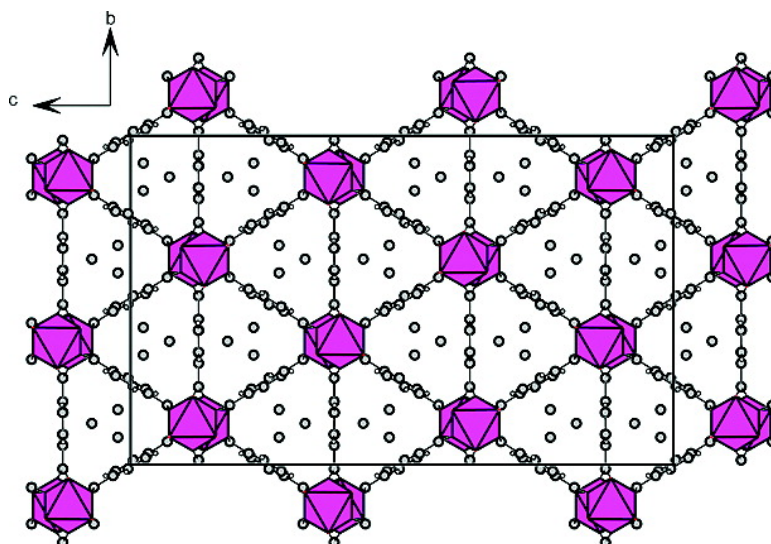


## Single Crystal X-ray Diffraction Studies of Carbon Dioxide and Fuel-Related Gases Adsorbed on the Small Pore Scandium Terephthalate Metal Organic Framework, Sc(OCCHCO)

Stuart R. Miller, Paul A. Wright, Thomas Devic, Christian Serre, Gerard Fey, Philip L. Llewellyn, Renaud Denoyel, Lucia Gaberova, and Yaroslav Filinchuk

*Langmuir*, 2009, 25 (6), 3618-3626 • DOI: 10.1021/la803788u • Publication Date (Web): 19 February 2009

Downloaded from <http://pubs.acs.org> on March 31, 2009



### More About This Article

Additional resources and features associated with this article are available within the HTML version:

- Supporting Information
- Access to high resolution figures
- Links to articles and content related to this article
- Copyright permission to reproduce figures and/or text from this article

[View the Full Text HTML](#)

# Single Crystal X-ray Diffraction Studies of Carbon Dioxide and Fuel-Related Gases Adsorbed on the Small Pore Scandium Terephthalate Metal Organic Framework, $\text{Sc}_2(\text{O}_2\text{CC}_6\text{H}_4\text{CO}_2)_3$

Stuart R. Miller,<sup>†</sup> Paul A. Wright,<sup>\*,†</sup> Thomas Devic,<sup>‡</sup> Christian Serre,<sup>‡</sup> Gérard Férey,<sup>‡</sup> Philip L. Llewellyn,<sup>§</sup> Renaud Denoyel,<sup>§</sup> Lucia Gaberova,<sup>§</sup> and Yaroslav Filinchuk<sup>||</sup>

School of Chemistry, University of St. Andrews, Purdie Building, North Haugh, St. Andrews, Fife, KY16 9ST, Institut Lavoisier, UMR CNRS 8180, 45, Avenue des Etats-Unis, Université de Versailles St-Quentin en Yvelines, 78035 Versailles, France, Laboratoire Chimie Provence, Universités d'Aix-Marseille I, II & III - CNRS, UMR 6264, Centre de Saint Jérôme, 13397 Marseille cedex 20, France, and SNBL, European Synchrotron Radiation Facility, 38043 Grenoble, France

Received November 14, 2008. Revised Manuscript Received January 12, 2009

The adsorption behavior of the microporous scandium terephthalate  $\text{Sc}_2(\text{O}_2\text{CC}_6\text{H}_4\text{CO}_2)_3$  for small fuel-related molecules has been measured. The structure shows an adsorption capacity for  $\text{N}_2$  and  $\text{CO}_2$  of  $6.5 \text{ mmol g}^{-1}$  and is able to take up straight chain hydrocarbons. The mechanism of adsorption of  $\text{CO}_2$ ,  $\text{CH}_4$ , and  $\text{C}_2\text{H}_6$  has been determined by single crystal synchrotron X-ray diffraction at  $\sim 230 \text{ K}$ . Adsorption of  $\text{CO}_2$  at  $235 \text{ K}$  and  $1 \text{ bar}$  pressure and  $\text{H}_2$  at  $80 \text{ K}$  and  $0.25 \text{ bar}$  results in each case in a symmetry change from orthorhombic  $Fddd$  to monoclinic  $C2/c$  through tilts in the terephthalate linkers.  $\text{CO}_2$  molecules take up different sites in the two symmetrically different channels that result from this symmetry change. The structure remains orthorhombic in  $9 \text{ bar}$  of  $\text{CH}_4$  and  $5 \text{ bar}$  of  $\text{C}_2\text{H}_6$ , and the adsorption sites are located.  $\text{CH}_4$  and  $\text{C}_2\text{H}_6$  are observed to adopt sites within the channels, and  $\text{C}_2\text{H}_6$  is also observed to adopt adsorption sites between phenyl groups in the channel walls, suggesting that the structure is sufficiently flexible to allow diffusion of small molecules between adjacent channels.

## Introduction

The selective adsorption of the greenhouse gas carbon dioxide is of importance for separation technologies that include the removal of  $\text{CO}_2$  from natural gas, the other components of which include light hydrocarbons ( $\text{CH}_4$ ,  $\text{C}_2\text{H}_6$ ) and  $\text{N}_2$ , the separation of  $\text{CO}_2$  from flue gases in power generation, and hydrogen purification, for example, of hydrogen generated by the water gas shift reaction. One target is a sorbent that permits good selectivity and a high reversible capacity between  $1$  and  $20 \text{ bar}$  or higher pressure at room temperature, the conditions for pressure swing adsorption (PSA) applications. Typical cationic zeolites have interactions with  $\text{CO}_2$  that are strong and, while good for removal of  $\text{CO}_2$  at low concentrations, would require thermal activation or vacuum for use in gas streams with high  $\text{CO}_2$  contents. Microporous metal organic frameworks,<sup>1–3</sup> MOFs, have been shown to possess promising properties for  $\text{CO}_2$  adsorption, including very high capacities<sup>4–6</sup> and the stepwise opening of flexible frameworks as seen for MIL-53 at elevated  $\text{CO}_2$  pressures (MIL = Material Institut Lavoisier).<sup>7,8</sup> The scandium terephthalate

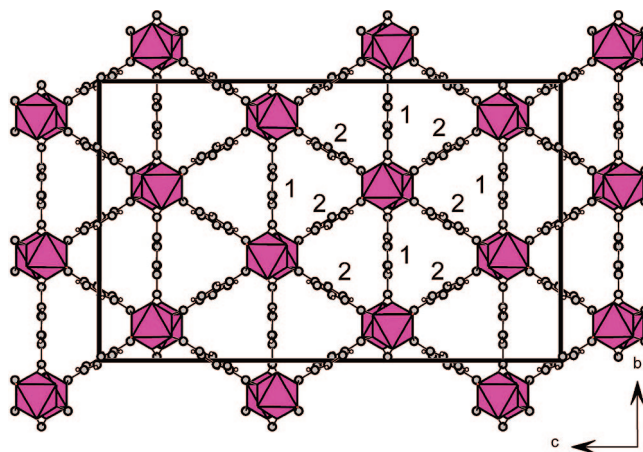


**Figure 1.** As-prepared small pore MOF ScBDC,  $\text{Sc}_2(\text{O}_2\text{CC}_6\text{H}_4\text{CO}_2)_3$ , viewed down the narrow channels, has orthorhombic symmetry. Crystallographically-distinct terephthalate groups are labeled 1 and 2.  $\text{ScO}_6$  octahedra are depicted in purple.

$\text{Sc}_2(\text{O}_2\text{CC}_6\text{H}_4\text{CO}_2)_3$ <sup>9,10</sup> (denoted here as ScBDC, Figure 1, BDC = 1,4-benzenedicarboxylate) is an attractive model sorbent for small molecules relevant to  $\text{CO}_2$  separation technologies. Although it contains small pores (ca.  $4 \text{ \AA}$  in free diameter), it has an adsorption capacity similar to that of the most porous zeolites because it has no inaccessible pore volume. It displays high thermal stability (up to ca.  $850 \text{ K}$  in nitrogen) and does not take up water molecules within its narrow pores, the geometry of which is such that adsorbed molecules experience van der Waals interactions with phenyl groups that make up the accessible

<sup>†</sup> University of St. Andrews.

<sup>‡</sup> Institut Lavoisier, UMR CNRS 8180.

<sup>§</sup> Universités d'Aix-Marseille I, II & III - CNRS, UMR 6264.

<sup>||</sup> SNBL, European Synchrotron Radiation Facility.

(1) Férey, G. *Chem. Soc. Rev.* **2008**, *37*, 191–214.

(2) Yaghi, O. M.; O'Keeffe, M.; Ockwig, N. W.; Chae, H. K.; Eddaoudi, M.; Kim, J. *Nature* **2003**, *423*, 705.

(3) Kitagawa, S.; Kitaura, R.; Noro, S. *Angew. Chem., Int. Ed.* **2004**, *43*, 2334.

(4) Millward, A. R.; Yaghi, O. M. *J. Am. Chem. Soc.* **2005**, *127*, 17998–17999.

(5) Llewellyn, P. L.; Bourrelly, S.; Serre, C.; Vimont, A.; Daturi, M.; Hamon, L.; De Weireld, G.; Chang, J.-S.; Hong, D.-Y.; Kyu Hwang, Y.; Hwa Jhung, S.; Férey, G. *Langmuir* **2008**, *24*, 7245–7250.

(6) Wang, B.; Côté, A. P.; Furukawa, H.; O'Keeffe, M.; Yaghi, O. M. *Nature* **2008**, *453*, 207–209.

(7) Bourrelly, S.; Llewellyn, P. L.; Serre, C.; Millange, F.; Loiseau, T.; Férey, G. *J. Am. Chem. Soc.* **2005**, *127*, 13519–13521.

(8) Llewellyn, P. L.; Bourrelly, S.; Serre, C.; Filinchuk, Y.; Férey, G. *Angew. Chem., Int. Ed.* **2006**, *45*, 7751–7754.

(9) Miller, S. R.; Wright, P. A.; Serre, C.; Loiseau, T.; Marrot, J.; Férey, G. *Chem. Commun.* **2005**, 3850–3852.

(10) Perles, J.; Iglesias, M.; Martin-Luengo, M. A.; Monge, M. A.; Ruiz-Valero, C.; Snejko, N. *Chem. Mater.* **2005**, *17*, 5837–5842.

pore walls, which are in close contact on all sides of the channel. These internal surfaces do not have uncoordinated metal sites or hydroxyl groups and do not require thermal treatment for removal of water molecules. We have therefore studied the adsorption of CO<sub>2</sub> and other small gas molecules on ScBDC to investigate the adsorption properties of a robust, crystallographically well-defined, small pore material with appreciable pore volume.

In addition to measuring adsorption isotherms, we have determined the location of selected adsorbate molecules in ScBDC by single crystal X-ray diffraction. Locating adsorbed molecules in microporous solids by diffraction-based methods is an important step toward understanding sorbent–sorbate interactions and ultimately in developing reliable interatomic potentials to simulate adsorption behavior. This route has been followed successfully in the location of adsorbed molecules in zeolites,<sup>11–13</sup> so that prediction of adsorption in these solids can now be considered routine. The same approach of diffraction and simulation is now being developed in the study of MOF adsorbents, including the location of CO<sub>2</sub> molecules adsorbed at hydroxyl sites.<sup>14</sup> The crystallographic determination of location and packing geometry of molecules in metal organic frameworks is important in understanding adsorption selectivities, as shown by Alaerts et al. for the uptake of xylene isomers in MIL-47.<sup>15</sup>

Where small molecules are physisorbed, without specific interactions, disorder over multiple positions is likely, so that low temperature diffraction studies are required to enable the sorbates to order at the most favorable sites. Examples include the location of hydrogen sites (as D<sub>2</sub>) on MOF-5 and other MOF materials by single crystal and powder neutron diffraction,<sup>16–18</sup> of Ar and N<sub>2</sub> on MOF-5 by single crystal X-ray diffraction,<sup>19</sup> and of O<sub>2</sub> in the small pores of a pillared layered coordination polymer, CPL-1, by X-ray powder diffraction.<sup>20</sup> For more specific interactions, such as NO molecules chemisorbed at uncoordinated metal cation sites<sup>21</sup> or acetylene hydrogen-bonded within the channels of a coordination polymer with a pillared layer structure,<sup>22</sup> adsorbates are localized at higher temperatures.

A preparation route described here gives pure and highly crystalline ScBDC in the form of crystals large enough for single crystal diffractometry. As a result, it has been possible to locate the sites of CO<sub>2</sub>, CH<sub>4</sub>, and C<sub>2</sub>H<sub>6</sub> adsorbed at temperatures of ~230 K within the pores, and the structure is observed to undergo



**Figure 2.** Single crystals of ScBDC prepared by the solvothermal method. Distance between the two black bars is 100 μm.

subtle structural rearrangement to accommodate CO<sub>2</sub> and H<sub>2</sub> molecules. These measurements have been related to adsorption isotherms.

## Experimental Section

**Synthesis of ScBDC via a Solvothermal Route.** Our previous work has shown that it is possible to prepare ScBDC hydrothermally.<sup>9</sup> In this work, it has been possible to improve the purity and crystal size by solvothermal synthesis. In a typical preparation, Sc(NO<sub>3</sub>)<sub>3</sub>·4H<sub>2</sub>O (Alfa Aesar, 0.34 g, 99.9%, 1.1 mmol), H<sub>2</sub>BDC (Aldrich, 0.170 g, 99%, 1 mmol), H<sub>2</sub>O<sub>2</sub> (Aldrich, 30 wt % in water, 0.25 mL), pyridine (Fisher, 0.5 mL, 99%), and dimethylformamide (DMF; Aldrich, 10 mL, 99.8%) were sealed in a Parr autoclave with a 23 mL Teflon liner. The mixture was subsequently heated to 493 K and allowed to react for 2 days. The autoclave was cooled, and the final product was filtered and washed with DMF. Large single crystals (~150 μm) were obtained (Figure 2). The purity of the solid was checked by powder X-ray diffraction on a STOE STADI/P diffractometer with a primary monochromator (Cu Kα<sub>1</sub>, 1.54056 Å) operating in Debye–Scherrer geometry. Thermogravimetric analysis (TGA) on the sample was performed in nitrogen, with an initial isothermal stage at 300 K followed by a heating ramp at 5 K min<sup>-1</sup> up to 1073 K. Single crystal diffraction of this material was performed in the laboratory at 93 and 298 K using a Rigaku diffractometer (Mo Kα) with a rotating anode (Table 1). The same crystal was used for both data collections, first at 298 K and then cooled to 93 K. Structures were solved using the SHELX software.<sup>23</sup> The higher residual (*R* = 9.1%) of the sample collected at 93 K is attributed to a small reduction in crystallinity upon cooling the crystal in a direct stream of cold nitrogen.

**Adsorption Manometry (100–300 K).** Adsorption isotherms were obtained up to 1 bar at various temperatures, using a commercial volumetric instrument (Coulter S.A.) in which the sample cell was adapted with a helium cryostat (CTI Cryogenics 8200). In this setup, it is possible to carry out adsorption experiments in the temperature

(11) Wright, P. A.; Thomas, J. M.; Ramdas, S.; Cheetham, A. K. *J. Chem. Soc., Chem. Commun.* **1984**, 1338–1339.

(12) Wright, P. A.; Thomas, J. M.; Cheetham, A. K.; Nowak, A. K. *Nature* **1985**, *318*, 611–614.

(13) Fitch, A. N.; Jobic, H.; Renouprez, A. *J. Phys. Chem.* **1986**, *90*, 1311–1318.

(14) Serre, C.; Bourelly, S.; Vimont, A.; Ramsahye, N. A.; Maurin, G.; Llewellyn, P. L.; Daturi, M.; Filinchuk, Y.; Leynaud, O.; Barnes, P.; Férey, G. *Adv. Mater.* **2007**, *19*, 2246.

(15) Alaerts, L.; Kirschhock, C. E. A.; Maes, M.; van der Veen, M. A.; Finsy, V.; Depla, A.; Martens, J. A.; Baron, G. V.; Jacobs, P. A.; Denayer, J. E. M.; De Vos, D. E. *Angew. Chem., Int. Ed.* **2007**, *46*, 4293–4297.

(16) Spencer, E. C.; Howard, J. A. K.; McIntyre, G. J.; Rowsell, J. L. C.; Yaghi, O. M. *Chem. Commun.* **2006**, 278–280.

(17) Peterson, V. K.; Liu, Y.; Brown, C. M.; Kepert, C. J. *J. Am. Chem. Soc.* **2006**, *128*, 15578–15579.

(18) Dincă, M.; Han, W. S.; Liu, Y.; Dailly, A.; Brown, C. M.; Long, J. R. *Angew. Chem., Int. Ed.* **2007**, *46*, 1419–1422.

(19) Rowsell, J. L. C.; Spencer, E. C.; Eckert, J.; Howard, J. A. K.; Yaghi, O. M. *Science* **2005**, *309*, 1350–1354.

(20) Matsuda, R.; Kitaura, R.; Kitagawa, S.; Kubota, Y.; Belosludov, R. V.; Kobayashi, T. C.; Sakamoto, H.; Chiba, T.; Takata, M.; Kawazoe, Y.; Mita, Y. *Nature* **2005**, *436*, 238–241.

(21) McKinlay, A. C.; Xiao, B.; Wragg, D. S.; Wheatley, P. S.; Megson, I. L.; Morris, R. E. *J. Am. Chem. Soc.* **2008**, *130*, 10440–10444.

(22) Kubota, Y.; Takata, M.; Matsuda, R.; Kitaura, R.; Kitagawa, S.; Kobayashi, T. C. *Angew. Chem., Int. Ed.* **2006**, *45*, 4932–4936.

(23) Sheldrick, G. M. *SHELX-97*; University of Göttingen: Germany, 1997.

**Table 1. Crystallographic Information of ScBDC As-Prepared and with Different Gases Adsorbed**

	as-prepared	as-prepared	CO <sub>2</sub>	H <sub>2</sub>	CH <sub>4</sub>	C <sub>2</sub> H <sub>6</sub>
formula unit	Sc <sub>2</sub> (BDC) <sub>3</sub>	Sc <sub>2</sub> (BDC) <sub>3</sub>	Sc <sub>2</sub> (BDC) <sub>3</sub> ·2CO <sub>2</sub>	Sc <sub>2</sub> (BDC) <sub>3</sub> ·xH <sub>2</sub>	Sc <sub>2</sub> (BDC) <sub>3</sub> ·CH <sub>4</sub>	Sc <sub>2</sub> (BDC) <sub>3</sub> ·2C <sub>2</sub> H <sub>6</sub>
<i>T</i>	93 K	298 K	235 K	80 K	230 K	230 K
adsorbate pressure			1 bar	0.25 bar	9 bar	5 bar
space group	<i>Fddd</i>	<i>Fddd</i>	<i>C2/c</i>	<i>C2/c</i>	<i>Fddd</i>	<i>Fddd</i>
X-ray source	Mo K $\alpha$	Mo K $\alpha$	SNBL, ESRF	SNBL, ESRF	SNBL, ESRF	SNBL, ESRF
wavelength (Å)	0.71070	0.71070	0.80926	0.80926	0.80926	0.71830
unit cell (Å)	orthorhombic <i>a</i> = 8.766(6) <i>b</i> = 20.795(13) <i>c</i> = 34.41(2)	orthorhombic <i>a</i> = 8.7503(11) <i>b</i> = 20.754(3) <i>c</i> = 34.366(4)	monoclinic <i>a</i> = 8.747(2) <i>b</i> = 34.464(8) <i>c</i> = 11.092(2) $\beta$ = 110.95° (3)	monoclinic <i>a</i> = 8.769(13) <i>b</i> = 34.4517(18) <i>c</i> = 11.1373(12) $\beta$ = 111.14(1)	orthorhombic <i>a</i> = 8.8001(3) <i>b</i> = 20.7921(5) <i>c</i> = 34.3972(6)	orthorhombic <i>a</i> = 8.8650(4) <i>b</i> = 20.7000(7) <i>c</i> = 34.3750(12)
<i>V</i> <sup>a</sup>	<i>V</i> = 6273(7) Å <sup>3</sup>	<i>V</i> = 6241(1) Å <sup>3</sup>	<i>V</i> = 3123(1) Å <sup>3</sup>	<i>V</i> = 3138(1) Å <sup>3</sup>	<i>V</i> = 6293(1) Å <sup>3</sup>	<i>V</i> = 6308(1) Å <sup>3</sup>
<i>Z</i> <sup>a</sup>	8	8	4	4	8	8
<i>R1</i> (all data)	0.1009	0.0518	0.0713	0.0375	0.0401	0.0519
<i>R1</i> ( <i>I</i> > 2 $\sigma$ <i>I</i> )	0.0918	0.0463	0.0684	0.0349	0.0352	0.0465
max and min residual e <sup>-</sup> density (e/Å <sup>3</sup> )	0.74, -0.86	0.41, -0.38	0.70, -0.67	0.20, -0.20	0.29, -0.27	0.69, -0.81

<sup>a</sup> *Z* is defined as the number of formula units per unit cell.

range from 30 to 300 K. Approximately 0.1 g of sample was outgassed under a constant residual vacuum pressure of  $5 \times 10^{-3}$  mbar using sample controlled thermal analysis (SCTA)<sup>24</sup> up to a final temperature of 423 K for 16 hours. A standard point-by-point dosing procedure was used for the adsorption and desorption experiments with a final pressure of 1 bar for the adsorption branch and 0.05 bar on desorption. Collection of the isotherm data was typically completed in around 24 hours.

**Adsorption Gravimetry at 303 K.** Adsorption experiments were carried out at 303 K up to 50 bars on a laboratory-made gas dosing system connected to a commercial gravimetric measuring system (Rubotherm Präzisionsmeßtechnik GmbH).<sup>25</sup> A step-by-step mode of gas introduction was used. Prior to each experiment, approximately 1 g of sample was outgassed to 423 K for 16 hours using the SCTA procedure above. Collection of the isotherm data was typically completed in around 12 hours.

**Adsorption Calorimetry: 77 and 303 K.** The calorimetry experiments were carried out using two different setups. Both calorimeters are of the isothermal Tian-Calvet type adapted to work at a nominal temperature of 77 or 303 K. The calorimeter used at 77 K consists of two thermopiles of around 800 thermocouples each, mounted in electrical opposition.<sup>26</sup> Around 150 mg of sample is placed inside the sample cell and inserted inside of the calorimeter after outgassing. The system is placed in the liquid cryostat filled with around 100 L of liquid nitrogen. A continuous procedure of nitrogen introduction is employed which is slow enough (approximately  $2 \text{ cm}^3 \text{ h}^{-1}$ ) to be close to equilibrium. This procedure leads to a high resolution in both the isotherm and differential enthalpies of adsorption. In this “quasi-equilibrium” state, the quantity of adsorbate admitted to the system  $\Delta n$  can be replaced by the rate of gas flow  $dn/dt$  which is kept constant by the use of a sonic nozzle. This gives the possibility of measuring  $\Delta_{\text{ads}}\hat{h}$  directly as a function of the amount adsorbed.

The experiments carried out at 303 K also use a Tian-Calvet type calorimeter (with over 1000 thermocouples in each thermopile) which is placed in a thermostat regulated to within 0.01 K.<sup>26</sup> Approximately 6 hours is required after introduction of the sample cell (ca. 300 mg) into the thermopile for thermal equilibrium to be attained. The adsorption isotherms are obtained using a homemade manometric device that permits measurement up to 100 bar. The point-by-point introduction of gas is most suitable for this system. Each introduction of adsorbate to the sample is accompanied by an exothermic thermal effect, until equilibrium is attained. This peak in the curve of energy with time is integrated to provide an integral (or pseudo-differential) molar enthalpy of adsorption for each dose. For each sample, the

values of  $\Delta_{\text{ads}}\hat{h}$  were obtained with a maximum error bar of 0.5 kJ mol<sup>-1</sup> over the whole pressure range. As for the other experiments, an SCTA procedure was used for outgassing as described above.

**SXRD of ScBDC with Adsorbed CO<sub>2</sub>, H<sub>2</sub>, CH<sub>4</sub>, and C<sub>2</sub>H<sub>6</sub>.** To examine the location of the lowest energy sites, single crystal experiments under controlled gas adsorbate pressures were performed at SNBL, ESRF, Grenoble. A single crystal of ScBDC was mounted on a glass fiber, which was then carefully introduced into a 0.3 mm quartz capillary and glued to it. The capillary was connected to a homemade vacuum/gas pressure controller and put on a goniometer head. The quality of the crystals was checked under vacuum, recording 20 frames at room temperature, until a suitable crystal was found.

Following evacuation, the crystal was exposed to gases at conditions of pressure and temperature chosen to permit the filling of sites at levels where the site occupancies are sufficiently high that the adsorbed molecules may be observed by diffraction. The single crystal data were therefore collected at 230 or 235 K for CO<sub>2</sub>, CH<sub>4</sub>, and C<sub>2</sub>H<sub>6</sub> and at pressures from 1 to 9 bar, values chosen based on the strength of the adsorption interaction as implied by the measured adsorption isotherms. In addition, single crystal diffraction data were also collected for a ScBDC crystal upon which H<sub>2</sub> was adsorbed at 80 K and 0.25 bar pressure, under which conditions ScBDC is known to adsorb  $\sim 6 \text{ mmol}(\text{H}_2) \text{ g}^{-1}$ .<sup>10</sup>

Pressure was kept constant during the whole data collection. A total of 175 frames were then collected at  $\lambda \approx 0.81 \text{ \AA}$  using the MAR-345 image plate detector. For ScBDC with adsorbed CO<sub>2</sub>, H<sub>2</sub>, CH<sub>4</sub>, and C<sub>2</sub>H<sub>6</sub>, good data sets were obtained. Data were processed using the CrysAlis software,<sup>27</sup> and structures were solved and refined using the SHELX program.<sup>22</sup> Crystallographic details of data collection of the as-prepared ScBDC and the gas-MOF complexes are summarized in Tables 1 and 2.

All gases used in these experiments were supplied by Air Liquide. The purity of nitrogen, oxygen, carbon monoxide, methane, and hydrogen were 99.9999% (N60), and the purity of carbon dioxide, ethane, and propane were 99.995% (N45).

**Crystallography. As-Prepared Sc<sub>2</sub>BDC<sub>3</sub> at 93 and 298 K.** The structures were solved and refined in the orthorhombic space group *Fddd* (no. 70). All non-hydrogen atoms were refined anisotropically, with hydrogen atoms being placed in calculated positions and refined using a riding model [*C*-H = 0.94 Å and *U*<sub>iso</sub>(H) = 1.2*U*<sub>eq</sub>(C)]. Any additional electron density observed in the as-prepared materials was negligible and located close to framework atoms. No additional electron density was observed within the pores of the material down to residual electron densities of 0.34 electrons/Å<sup>3</sup> (at 93 K) and 0.18 electrons/Å<sup>3</sup> (at 298 K).

**Sc<sub>2</sub>BDC<sub>3</sub> with Adsorbed Gas Molecules.** Prior to collecting data sets on ScBDC in the presence of different gases, a unit cell matrix

(24) Rouquerol, J. *Thermochim. Acta* **1989**, *144*, 209–224.

(25) De Weireld, G.; Frère, M.; Jadot, R. *Meas. Sci. Technol.* **1999**, *10*, 117–126.

(26) Llewellyn, P. L.; Maurin, G. C. R. *Chimie* **2005**, *8*, 283–302.

(27) *CrysAlisProCCD and CrysAlisProRED*; Oxford Diffraction Ltd.: Abingdon, Oxfordshire, England, 2006.

**Table 2. Structural Details of ScBDC as a Function of Gas Adsorption, Including Tilt Angles to Channel Axis, Torsion Angles between Carboxylate and Phenyl Groups in the Terephthalate Rings, and Dimensions of Gaps between Phenyl Groups in the Channel Walls**

	as-prepared	as-prepared	CO <sub>2</sub>	H <sub>2</sub>	CH <sub>4</sub>	C <sub>2</sub> H <sub>6</sub>
approx. formula	Sc <sub>2</sub> (BDC) <sub>3</sub>	Sc <sub>2</sub> (BDC) <sub>3</sub>	Sc <sub>2</sub> (BDC) <sub>3</sub> ·2CO <sub>2</sub>	Sc <sub>2</sub> (BDC) <sub>3</sub> ·xH <sub>2</sub>	Sc <sub>2</sub> (BDC) <sub>3</sub> ·CH <sub>4</sub>	Sc <sub>2</sub> (BDC) <sub>3</sub> ·2C <sub>2</sub> H <sub>6</sub>
<i>T</i> , <i>P</i> (gas)	93 K, –	298 K, –	235 K, 1 bar	80 K, 0.25 bar	230 K, 5 bar	230 K, 5 bar
group 1 tilt to channel (°)	0	0	0	0	0	0
group 2a tilt to channel (°)	8.0(1)	7.9(1)	5.8(1)	4.3(2)	6.7(1)	1.5(1)
group 2b tilt to channel (°) <sup>a</sup>	8.0(1)	7.9(1)	13.8(2)	11.3(2)	6.7(1)	1.5(1)
group 1 torsion angle (°)	17.1(7)	17.8(3)	17.5(8)	17.9(5)	17.7(4)	17.8(5)
group 2a torsion angle (°)	1.5(8)	1.9(4)	11.5(8)	1.9(5)	2.9(4)	6.7(5)
group 2b torsion angle (°)	1.5(8)	1.9(4)	0.7(9)	2.2(5)	2.9(4)	6.7(5)
group 1 to group 1 distance (Å)	5.305(3)	5.290(1)	4.94(4)	4.97(2)	5.360(1)	5.449(1)
group 2a to group 2a (Å)	4.435(3) <sup>a</sup>	4.423(1) <sup>a</sup>	4.25(1)	4.269(8)	4.447(1) <sup>a</sup>	4.453(1) <sup>a</sup>
group 2b to group 2b (Å)	4.435(3) <sup>a</sup>	4.423(1) <sup>a</sup>	4.65(5)	4.55(2)	4.447(1) <sup>a</sup>	4.453(1) <sup>a</sup>

<sup>a</sup> For orthorhombic structures, groups 2a and 2b are symmetrically equivalent.

was collected on the as-prepared material under vacuum, which showed that the cell could be indexed as the orthorhombic (*Fddd*) cell observed in the laboratory measurements. The crystal was then subject to different gas environments (Table 2), ensuring the capillary was evacuated completely between different gas environments.

The crystal adopted either orthorhombic (*Fddd*) or monoclinic (*C2/c*, no. 15) symmetry, depending upon the pressure and type of gas that was adsorbed. In experiments with CH<sub>4</sub> and C<sub>2</sub>H<sub>6</sub>, the structure was orthorhombic, and in the presence of CO<sub>2</sub> and H<sub>2</sub> it was monoclinic. Regardless of the crystal system, all framework atoms were refined anisotropically, with hydrogen atoms being placed in calculated positions and refined using a riding model [*C*–*H* = 0.94 Å and *U*<sub>iso</sub>(*H*) = 1.2*U*<sub>eq</sub>(*C*)]. Additional electron density was located within the one dimensional channels of the material in the case of CO<sub>2</sub> and CH<sub>4</sub>, and located both within and between channels in the case of C<sub>2</sub>H<sub>6</sub>. No additional electron density could be reliably allocated to extra framework hydrogen in the case of H<sub>2</sub> adsorption.

In all cases, atoms of gas species adsorbed within the material were refined isotropically. In the case of the CO<sub>2</sub>, the total uptake could be estimated from the measured adsorption isotherms (see later) at ~3.5 mmol g<sup>-1</sup>. Two positions were found for CO<sub>2</sub>, one of which could only be occupied to a maximum of 50% because of close atom–atom contacts. Maximum possible occupancy of these sites (full occupancy of one site and 50% of the other) gave an uptake of 3.4 mmol g<sup>-1</sup>, close to that predicted from the adsorption isotherms. This gives the same density of CO<sub>2</sub> molecules in each of the two channels and a total uptake of 8 molecules of CO<sub>2</sub> per monoclinic unit cell.

For the structure of ScBDC with CH<sub>4</sub> adsorbed at 230 K at a pressure of 9 bar, no direct measurement of uptake was available due to current instrument limitations. However, the adsorption isotherm was measured up to 1 bar at the temperature of the diffraction experiment. The adsorption isotherm (Supporting Information) could be fitted well from 0.3 to 0.7 mmol g<sup>-1</sup> according to a Langmuir isotherm, from which an uptake of ~1.7 mmol g<sup>-1</sup> is predicted at 9 bar and 230 K by extrapolation. Taking this as a reasonable estimate of the uptake in the diffraction experiment, the sum of the occupancies of carbon atoms at the two located CH<sub>4</sub> sites, C8 and C9, was constrained to give this value, and the displacement parameters were allowed to refine freely. In each of the two sites, there were four molecules of CH<sub>4</sub> per unit cell, giving a total uptake of eight molecules per orthorhombic unit cell.

For the C<sub>2</sub>H<sub>6</sub> adsorption, the largest nonframework peaks were attributed to C<sub>2</sub>H<sub>6</sub> carbon atoms. For the strongest peaks, carbon atoms were refined with displacement parameters equal to those assigned to the carbon atoms of CH<sub>4</sub> molecules in the SCBDC–CH<sub>4</sub> experiment performed at the same temperature. The electron density was best fitted by ethane molecules located in two regions in the structure, and in each of these two regions the ethane molecules were best modeled by being disordered over two very close sites. An estimate of the C<sub>2</sub>H<sub>6</sub> content was made from summing the refined occupancies, so that the “channel” sites (see later) were fully occupied (8 per orthorhombic unit cell) and the “wall” sites were a little over 50% occupied (8.4 per unit cell). A

total loading of 16.4 C<sub>2</sub>H<sub>6</sub> molecules per orthorhombic unit cell was measured in this way (3.5 mmol g<sup>-1</sup>).

## Results and Discussion

**Synthesis and Characterization.** The solvothermal synthesis route gives highly crystalline, phase pure ScBDC, as shown by the indexed laboratory X-ray powder diffraction pattern (Supporting Information). The product is made up of large single crystals 150 μm in size. Thermogravimetric analysis indicates that there is no solvent left in the pores and the structure is stable in nitrogen up to ~850 K (Supporting Information). Single crystal analysis confirms that the structure is as previously reported and that it is almost identical at 93 K and room temperature, with no significant electron density measured in the pores (Table 1). There are two crystallographically distinct terephthalate groups in the structure, labeled 1 and 2 in Figure 1, and there are twice as many groups of type 2 as there are of type 1. The average angle made by the plane of the –CO<sub>2</sub> group of the terephthalate linker with the plane of the phenyl ring is ~17° for groups of type 1 and ~2° for groups of type 2, and groups 1 and 2 are tilted with respect to that channel axis by 0° and 8°, respectively.

Nitrogen adsorption at 77 K gives a type I isotherm, with a maximum uptake of 6.5 mmol g<sup>-1</sup> corresponding to a pore volume of ~0.23 cm<sup>3</sup> g<sup>-1</sup>, close to that reported previously (Supporting Information). This value is comparable to the accessible pore volumes of zeolites (e.g., zeolite β, 0.22 cm<sup>3</sup> g<sup>-1</sup>; ITQ-29, the pure silica version of zeolite A, 0.24 cm<sup>3</sup> g<sup>-1</sup>) but is much lower than those of the more porous MOF materials (e.g. MIL-101, 1.96 cm<sup>3</sup> g<sup>-1</sup>; MOF-177, 1.59 cm<sup>3</sup> g<sup>-1</sup>).<sup>28</sup> The more remarkable feature of the material is therefore that all adsorbed molecules are close to the framework on all sides.

Initial heats of adsorption of N<sub>2</sub> (0–3 mmol g<sup>-1</sup>) are in the range 18–19 kJ mol<sup>-1</sup> and decrease as pore filling is approached, presumably as repulsive interactions become important within a denser packing regime. This enthalpy is comparable with those obtained on electrically neutral pure silica “zeolites” where no specific interactions occur. Thus, the enthalpy obtained with ScBDC is slightly higher than that obtained for purely siliceous zeolites such as silicalite (*d*<sub>pore</sub> ≈ 6 Å, –15 kJ mol<sup>-1</sup>)<sup>29</sup> or dealuminated Y (*d*<sub>cage</sub> ≈ 12 Å, –12 kJ mol<sup>-1</sup>),<sup>30</sup> which may be due to a higher degree of confinement in the MOF with respect to these zeolites. The enthalpy of adsorption for nitrogen adsorption in other MOFs has not often been reported: the

(28) Wright, P. A. *Microporous Framework Solids*; RSC Publishing: Cambridge, 2007; pp 261–262.

(29) Llewellyn, P. L.; Coulomb, J.-P.; Grillet, Y.; Patarin, J.; André, G.; Rouquerol, J. *Langmuir* **1993**, *9*, 1852–1856.

(30) Llewellyn, P. L.; Maurin, G.; Poyet, T.; Dufau, N.; Denoyel, R.; Rouquerol, F. *Adsorption* **2005**, *11*, 73–78.

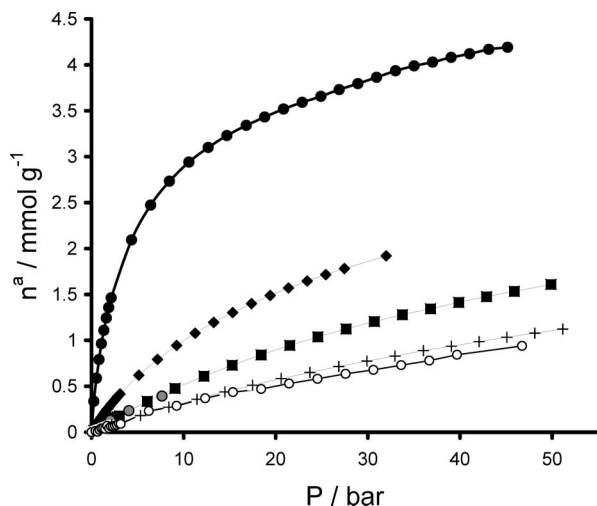


**Figure 3.** Adsorption isotherms of fuel-related gases on ScBDC at 304 K and up to 50 bar, measured gravimetrically. (Black circles, CO<sub>2</sub>; black tilted squares, CH<sub>4</sub>; black squares, O<sub>2</sub>; gray circles, CO; crosses, N<sub>2</sub>; open circles, H<sub>2</sub>.)

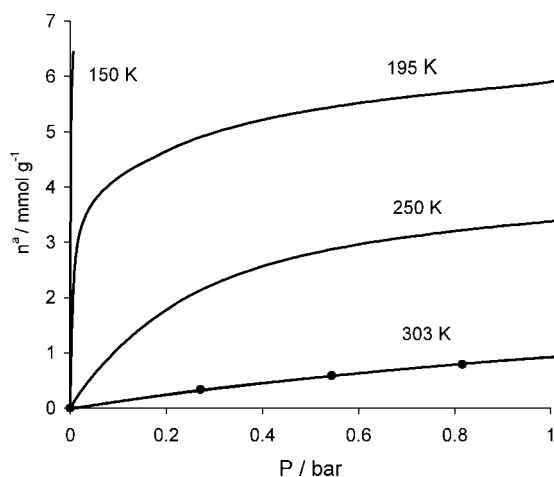


**Figure 4.** Adsorption isotherms from 0 to 1 bar for CO<sub>2</sub> on ScBDC at temperatures between 150 and 303 K. Solid lines were data measured volumetrically. For the 303 K data points, obtained gravimetrically are plotted for comparison.

magnitudes of enthalpies on ScBDC are slightly higher than those obtained on the large pore Ni phosphonate MOF, STA-12 ( $d_{\text{pore}} \approx 8 \text{ \AA}$ ,  $-16 \text{ kJ mol}^{-1}$ ; STA = St. Andrews microporous material).<sup>31</sup>

**Adsorption Behavior for Fuel-Related Gases.** Room temperature adsorption of selected inorganic gases (CO<sub>2</sub>, CO, O<sub>2</sub>, N<sub>2</sub>, H<sub>2</sub>) up to pressures of 50 bar (Figure 3) indicates that the uptake of CO<sub>2</sub> is the highest in terms of both mmol g<sup>-1</sup> and g g<sup>-1</sup>, approaching 4.5 mmol g<sup>-1</sup> at 50 bar. The reversible capacity for CO<sub>2</sub> at 304 K between 1 and 50 bar is 3.4 mmol g<sup>-1</sup>. Adsorption isotherms up to 1 bar total pressure were also measured at different temperatures for CO<sub>2</sub> (Figure 4). For CO<sub>2</sub>, the maximum uptake is  $\sim 6.5 \text{ mmol g}^{-1}$ , achieved both at 1 bar at 195 K, the boiling point of CO<sub>2</sub>, and at 0.006 bar ( $p/p_0 = 1$ ) at 150 K.

Calorimetric measurement of the differential heats of adsorption of CO<sub>2</sub> at room temperature at low loadings (up to 1 mmol g<sup>-1</sup>) gives values around 20 kJ mol<sup>-1</sup> (Figure 5), much lower than those for adsorption on cationic zeolites, such as NaX (40–45

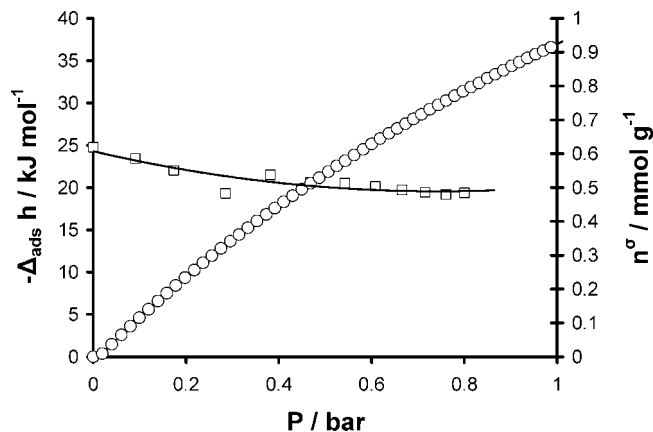


**Figure 5.** Adsorption isotherm (open circles) and differential heats of adsorption (open squares) of CO<sub>2</sub> on ScBDC at 304 K and up to 1 bar.

kJ mol<sup>-1</sup>) and similar to interaction energies with nonpolar silicas, such as dealuminated Y (17–23 kJ mol<sup>-1</sup>).<sup>32</sup> The heat of adsorption for CO<sub>2</sub> on the ScBDC is much lower than that observed for the large pore MOFs MIL-100 (60 kJ mol<sup>-1</sup>) or MIL-101 (45 kJ mol<sup>-1</sup>) which is due to the presence of coordinatively unsaturated sites in the latter materials.<sup>33</sup> A comparison with MOFs other than MIL-101 with the BDC linker but without coordinatively unsaturated sites is also possible. In the case of MIL-53 (Cr or Al) an initial adsorption enthalpy of around  $-35 \text{ kJ mol}^{-1}$  is observed which may be due to the interaction with the  $-\text{OH}$  group on the metal.<sup>34</sup> However, on MIL-47 (V), where no specific adsorption site is present, an initial adsorption energy of around  $-20$  to  $-25 \text{ kJ mol}^{-1}$  is observed (in the same range as observed here).<sup>34</sup> It would seem that no strong confinement effect, with higher adsorption enthalpy, is observed for CO<sub>2</sub> on ScBDC.

Among the other inorganic gases, the uptake of oxygen (O<sub>2</sub>) is greater than that of nitrogen (N<sub>2</sub>), indicating that the smaller size of O<sub>2</sub> (kinetic diameter 3.46 Å cf. 3.64 Å<sup>35</sup>) is more important than the greater polarizability and larger quadrupole moment of N<sub>2</sub>. The uptake of carbon monoxide is similar to that of O<sub>2</sub>, indicating there is only weak interaction between the CO dipole and the framework. CO is adsorbed less strongly than CH<sub>4</sub>, as expected for adsorption on a nonpolar sorbent. H<sub>2</sub> adsorption reaches less than 1 mmol g<sup>-1</sup>, even at 50 bar, even though this material is known to fill with hydrogen at 77 K, giving a maximum uptake of 6.75 mmol g<sup>-1</sup>.

The adsorption isotherms of the small alkanes methane, ethane, and propane, C<sub>3</sub>H<sub>8</sub>, are compared in Figure 6. The adsorption of all these molecules, including C<sub>3</sub>H<sub>8</sub>, indicates that the pore size is sufficient for access of linear hydrocarbons (ca. 4 Å). Calorimetric measurement of the heat of adsorption of methane gives values from 17 to 14 kJ mol<sup>-1</sup> at loadings of 0.1 to 0.5 mmol g<sup>-1</sup> (Supporting Information). These are similar to those measured on the phosphonate MOF, Ni STA-12. It is noteworthy that the heat of adsorption of CO<sub>2</sub> is higher for Ni STA-12 (33 kJ mol<sup>-1</sup>) than for ScBDC due to the presence of coordinatively unsaturated metal sites: as a result, Ni STA-12 shows a higher

(32) Maurin, G.; Llewellyn, P. L.; Bell, R. G. *J. Phys. Chem. B* **2005**, *109*, 16084–16091.

(33) Llewellyn, P. L.; Bourelly, S.; Serre, C.; Vimont, A.; Daturi, M.; Hamon, L.; De Weireld, G.; Chang, J. S.; Hong, D.-Y.; Hwang, Y. K.; Jung, S. H.; Férey, G. *Langmuir* **2008**, *24*, 7245–7250.

(34) Bourelly, S.; Llewellyn, P. L.; Serre, C.; Millange, F.; Loiseau, T.; Férey, G. *J. Am. Chem. Soc.* **2005**, *127*, 13519–13521.

(35) Breck, D. W. *Zeolite Molecular Sieves: Structure, Chemistry and Uses*; Wiley: New York, 1973; p 626.

(31) Miller, S. R.; Pearce, G. M.; Wright, P. A.; Bonino, F.; Chavan, S.; Bordiga, S.; Margiolaki, I.; Guillou, N.; Férey, G.; Bourrelly, S.; Llewellyn, P. L. *J. Am. Chem. Soc.* **2008**, *130*, 15967–15981.

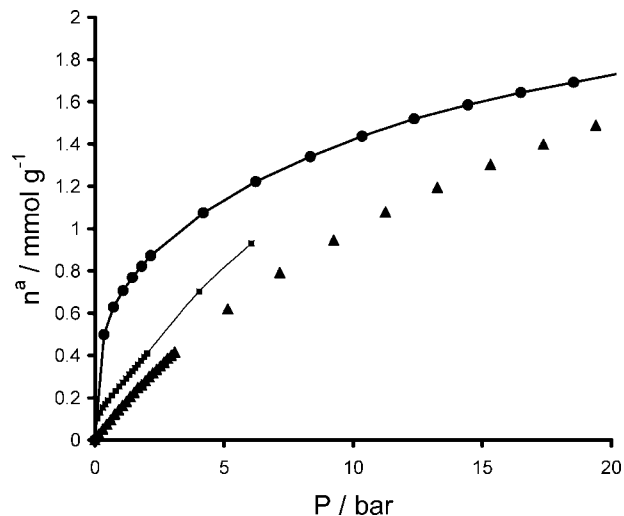


**Figure 6.** Adsorption isotherms at 304 K for small alkanes on ScBDC measured gravimetrically. (Closed triangles, CH<sub>4</sub>; closed circles, C<sub>2</sub>H<sub>6</sub>; closed squares, C<sub>3</sub>H<sub>8</sub>.)

ratio of CO<sub>2</sub>/CH<sub>4</sub> uptake than ScBDC. At 1 bar and 304 K, the ratio is ca. 10 for Ni STA-12, compared to ca. 6 for ScBDC.<sup>31</sup>

**Structural Studies of Adsorption.** To investigate the location of adsorbed molecules, single crystals of ScBDC were evacuated, cooled to 230 K, and then put into contact with CO<sub>2</sub>, CH<sub>4</sub>, and C<sub>2</sub>H<sub>6</sub> at 1, 9, and 5 bar, respectively. In addition, the crystal structure was also measured in H<sub>2</sub> at 80 K and 0.25 bar. Structural details are given in Tables 1 and 2.

**ScBDC–CO<sub>2</sub> (235 K; 1 bar).** Carbon dioxide was adsorbed on a crystal of scandium terephthalate at 235 K and 1 bar, under which conditions an uptake of ~3.5 mmol g<sup>-1</sup> is expected from the measured isotherms, corresponding to around two molecules of CO<sub>2</sub> per Sc<sub>2</sub>(O<sub>2</sub>CC<sub>6</sub>H<sub>4</sub>CO<sub>2</sub>)<sub>3</sub> unit. The symmetry has changed to monoclinic, *C2/c*, as a result of this CO<sub>2</sub> adsorption. There are three different terephthalate groups in this symmetry: group 1, corresponding to group 1 of the orthorhombic structure, and groups 2a and 2b, which result from loss of degeneracy of groups of type 2 of the orthorhombic structure as the symmetry is lowered (Figure 7A). The structural change results in rotation of one of the terephthalate groups (2b) by 14° away from the *a* axis (compared to 8° in the orthorhombic form and 5.8° for group 2a). As a consequence of this rotation and the change in symmetry, the structure has two different types of triangular channels, which alternate in rows perpendicular to the *b* axis (Figure 7A). The cause of this change is the adsorption of CO<sub>2</sub> molecules, which occupy two different sites within the two different types of channels, denoted A and B: these environments are shown in Figure 7B and C. Details of the CO<sub>2</sub> adsorption sites are given in Table 3.

In channel A, the occupancy is close to 1, and the CO<sub>2</sub> molecule's axis is aligned so that the oxygen atoms of the C=O groups point toward the H atoms of framework phenyl groups, giving O···H distances of 2.87 and 2.89 Å. Within channel B, where the effect of the linker on the geometry of the channel pore space is most marked, there are two symmetry-related sites, which are too close (O···O distance 2.2 Å) to allow simultaneous occupation of the two sites. The shortest distances (all OCO–H) are 2.78, 2.92, and 2.98 Å. These are longer than the –O···HC≡CH nonbonded distances observed by Kubota et al for acetylene adsorbed on the M phase of the coordination polymer CPL-1, ~2.6 Å, indicating the CO<sub>2</sub>···ScBDC interaction is relatively weak.<sup>22</sup> Examination of the geometry around the CO<sub>2</sub> molecule indicates that in the monoclinic form the phenyl

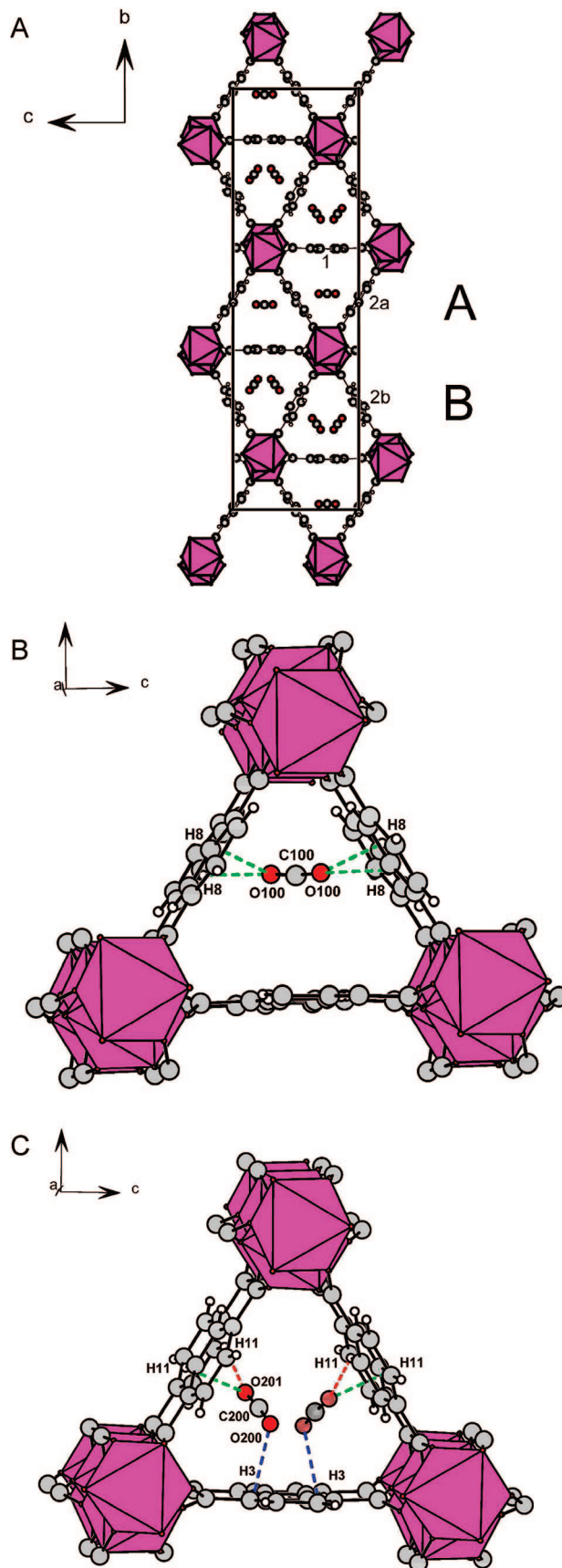


**Figure 7.** (A) Sites of CO<sub>2</sub> molecules adsorbed in ScBDC at 1 bar and 235 K, viewed down the channel axes. Note that in rows of channels of type A and B the channels are no longer identical due to the different rotation of the terephthalate groups of type 2a and 2b. The environments of CO<sub>2</sub> in the triangular pores in channels of types A and B are illustrated in more detail in (B) and (C), respectively.

**Table 3. Details of CO<sub>2</sub> Adsorption Sites in ScBDC at 235 K and 1 bar CO<sub>2</sub> Pressure**

	CO <sub>2</sub> atom labels	site multiplicity (unit cell)	fractional site Occupancy	distances of nearest approach to framework (Å)
site 1	O100–C100–O100	4	1.0	O100···H8 2.88
site 2	O200–C200–O201	8	0.5	O200···H3 2.87 O201···H11 2.93 O201···H11 2.98

groups of type 2b have reoriented so that channel B becomes more of a cavity structure. One aromatic group moves to be parallel to the axis of the CO<sub>2</sub> molecule and one of the OCO

**Table 4. Details of CH<sub>4</sub> Adsorption Sites in ScBDC at 230 K and 9 bar CH<sub>4</sub>**

	CH <sub>4</sub> carbon atom label	site multiplicity (unit cell)	fractional site occupancy	distances of nearest approach to framework (Å)
site 1	C8	16	0.25	C8···H32.94 C8···H33.22
site 2	C9	32	0.125	C9···H72.79 C9···H62.98 C9···H73.03

oxygen atoms points towards a H atom of the next tilted phenyl ring along the channel.

Maximum possible occupancy of CO<sub>2</sub> in the measured sites in channels A and B without unreasonably close O···O distances

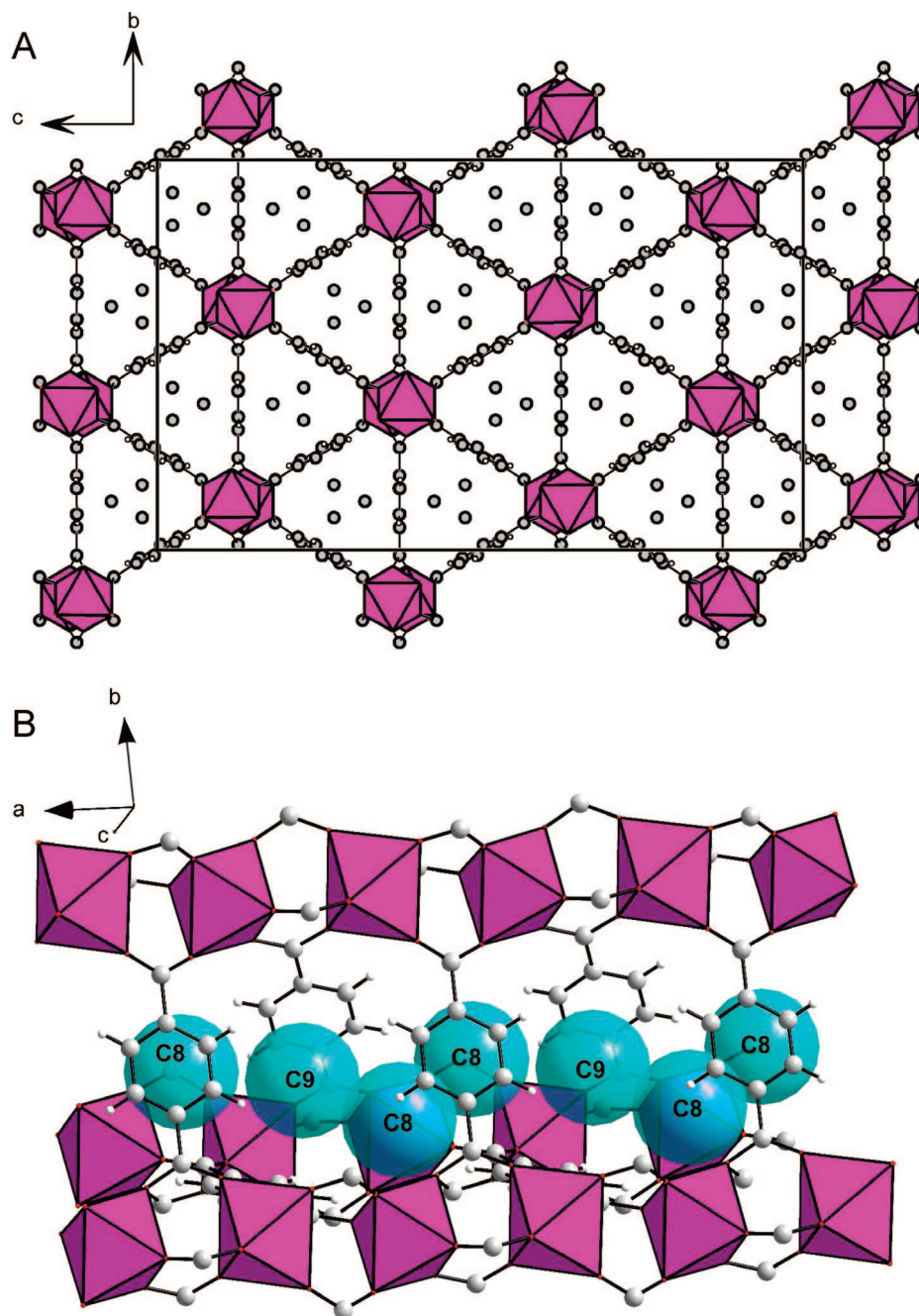


**Figure 8.** (A) Methane C atom positions in ScBDC viewed down the channel axis. The location of the two sites found for methane C atoms C8 and C9 in the channels are shown in (B), viewed perpendicular to the *a* axis.



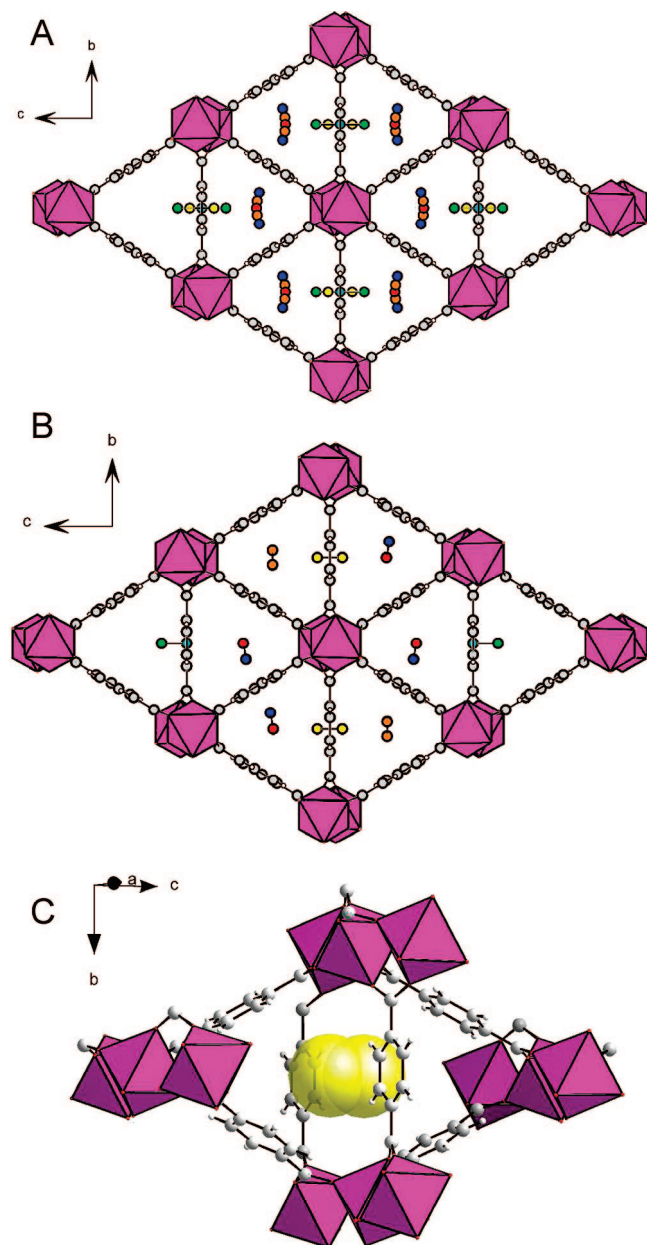


**Figure 9.** (A, B) For  $C_2H_6$  adsorbed at 230 K and 5 bar, ethane C atoms are in two types of sites. These are within the channels (blue, orange, red) and in gaps between phenyl groups in the wall (green, yellow, cyan). In each type of site, the ethane molecule C–C groups are disordered over two sites (blue–red, orange–orange and green–cyan, yellow–yellow). In (B), one possible arrangement of molecules is shown (as C atoms only). The location of ethane molecules between phenyl groups is illustrated (with partially transparent C atoms with van der Waals radii in yellow) in (C).

gives a total  $CO_2$  loading of  $3.4 \text{ mmol g}^{-1}$ , which is reasonably close to the value predicted from the isotherms at 1 bar (at 250 K and 1 bar, the measured uptake is  $3.4 \text{ mmol g}^{-1}$ , and at 230 K it will be slightly higher). Notably, at higher pressure or lower temperature, the  $CO_2$  loading can be increased, to a maximum of  $6.5 \text{ mmol g}^{-1}$ . This must result in a slight modification of the packing arrangement to avoid the unfavorable intermolecular interactions.

The sizes of the openings perpendicular to the main channels between phenyl groups along the  $a$  direction (Table 2) have changed, so that the distances between hydrogen atoms of adjacent groups of types 1, 2a, and 2b that limit molecular passage are 4.95, 4.25, and 4.67 Å, respectively. For  $CO_2$ , which has a two-

center Lennard–Jones diameter of 3 Å,<sup>36</sup> this suggests that there is enough space, even if van der Waals radii of the H atoms are taken into account, for  $CO_2$  to move between adjacent channels of type A and B (in between groups of type 1) but that motion along the layers of A and B channels or indeed three dimensional diffusion of  $CO_2$  would be more difficult, requiring considerable phenyl group rotation.

**ScBDC– $H_2$  (80 K; 0.25 bar).** The crystal structure of ScBDC containing  $H_2$  was also found to adopt monoclinic  $C2/c$  symmetry, but it was not possible to locate the  $H_2$  molecules unambiguously. The same mode of framework distortion that is observed for the  $CO_2$  uptake has occurred to accommodate the  $H_2$  molecules, although the torsion angles and degrees of tilt are different (Table 2). This suggests that the cause of the distortion is related to the packing of adsorbed  $H_2$  (and  $CO_2$ ) in the pores and the steric effects of their confinement, rather than the magnitude of their enthalpic interaction.

**ScBDC– $CH_4$  (230 K; 9 bar).** The crystal structure of ScBDC in equilibrium with  $CH_4$  gas at 230 K and 9 bar was found to display orthorhombic  $Fddd$  symmetry.  $CH_4$  molecules are located in the pores, with low occupancies and high displacement parameters ( $0.072(6) \text{ \AA}^2$ ). Two positions are located for their C atoms, C8 and C9, with nearest distances between them and the H atoms of the framework being reasonable, at 2.8–3.2 Å (Table 4 and Figure 8). The sum of the van der Waals distances of  $CH_4$  (1.85 Å) and H (1.2 Å) is  $\sim 3.05 \text{ \AA}$ .<sup>35,36</sup> Smaller values than this observed for nonbonded C···H distances (e.g., C9···H7, 2.79 Å) may be explained by the low occupancy of the methane molecules and the high displacement parameters of the methane carbon atom. The observed position of the phenyl groups is an average value, which will be dominated by the groups without adjacent methane molecules, whereas those groups next to methane molecules are likely to be slightly displaced. Both sites are located opposite a phenyl ring on one side and fitting into the gap between rings on the other. The distances between methane molecules in the closest symmetry-related C9 sites are too close (2.96 Å) for them to be occupied simultaneously. Other methane–methane distances (C8···C8, 3.66 Å; C8···C9, 3.71 Å; and C9···C9, 3.82 Å) are close to or slightly below the van der Waals diameter of methane, 3.73 Å.<sup>36</sup> Occupying all these sites with close approaches from 3.66 to 3.82 Å would give a maximum uptake of  $6.8 \text{ mmol g}^{-1}$ .

**ScBDC– $C_2H_6$  (230 K; 5 bar).** Single crystal diffraction of ScBDC with ethane adsorbed was also performed at 230 K, with an equilibrium pressure of 5 bar. The structure remains orthorhombic, but there is an expansion of around 0.1 Å along the channel axis, parallel to the chains of  $ScO_6$  octahedra, compared to the other structures.  $C_2H_6$  is located in two types of sites, with the first within the channels between aromatic rings and the second with the molecule bridging between adjacent channels, located in the gap between phenyl rings in the channel walls. In each case,  $C_2H_6$  is best modeled by two crystallographically distinct positions slightly displaced from each other: these positions are shown in Figure 9A and B. The total ethane occupancies in these two sites are similar (8 molecules per unit cell per type of site) giving an estimated loading of  $3.5 \text{ mmol g}^{-1}$ . For the second site, between phenyl groups of type 1 in the wall, the distance between diametrically opposite phenyl hydrogen atoms is sufficiently large (5.45 Å) to allow the location, and presumably the passage, of  $C_2H_6$  (which has a two-center Lennard–Jones diameter of 3.5 Å).<sup>36</sup> It is likely, however, that the distance between rings across the gap in the other type of channel wall would, at 4.5 Å, be too short to allow passage of

(36) Vrabec, J.; Stoll, J.; Hasse, H. *J. Phys. Chem. B* **2001**, *105*, 12126–12133.

C<sub>2</sub>H<sub>6</sub>, although it may be that thermal motion of the rings could allow the amount of opening that is required.

### Conclusions

The scandium terephthalate ScBDC has a small pore structure that interacts weakly with water, so it does not require thermal activation prior to use. It adsorbs CO<sub>2</sub> more strongly than CH<sub>4</sub>, C<sub>2</sub>H<sub>6</sub>, or C<sub>3</sub>H<sub>8</sub>, but the heat of adsorption is moderate (ca. 20 kJ mol<sup>-1</sup>) so that the uptake is readily reversible.

Well-defined adsorption sites for physisorbed CO<sub>2</sub>, CH<sub>4</sub>, and C<sub>2</sub>H<sub>6</sub> have been measured on large single crystals of ScBDC prepared solvothermally, using an environmental cell working at adsorbate gas pressures of 1–10 bar. In this way, it has been possible to obtain details of the adsorption mechanism of ScBDC, which is a model small pore MOF for which the constraints imposed by the pore structure on packing of even small molecules of different shape are of great importance. For CH<sub>4</sub> and C<sub>2</sub>H<sub>6</sub>, the framework structure is closely similar to that of the as-prepared solid and the adsorbed molecules fit closely to the available pore space. In the case of the C<sub>2</sub>H<sub>6</sub>, the molecule is able to adopt two types of sites, one in the channel and one bridging between two channels via a gap in the channel wall between two phenyl groups.

For both CO<sub>2</sub> and H<sub>2</sub> adsorption, the structure adapts by ligand rotation resulting in two different channel types. For the CO<sub>2</sub> adsorption, this permits end-on interaction of CO<sub>2</sub> oxygen atoms with framework aromatic H atoms, and in one of the sites the phenyl rings rotate to make a cavity in which three phenyl groups rotate to be close to parallel to the linear CO<sub>2</sub> molecule, forming

a “collar” around it, while the CO<sub>2</sub> molecule also interacts end-on with a phenyl ring hydrogen further along the channel.

ScBDC is therefore able to adsorb a range of small molecules, including those relevant to fuel technologies. CO<sub>2</sub> is adsorbed more strongly than light hydrocarbons and CO, and ongoing studies are investigating shape selective exclusion as molecules of larger size are put into contact with this solid. The material is ideally suited for the location of physisorbed molecules, because it can be prepared as large crystals and the pore diameters are small enough to permit localization without chemisorption, even at temperatures of 230 K. Furthermore, the narrow pores of this MOF provide a critical test of intermolecular potentials that we are developing to model adsorption isotherms computationally.

**Acknowledgment.** We gratefully acknowledge financial support from the EC STREP program “DeSANNs” (SES6-CT-2005-020133) and the ESRF for providing access to the Swiss-Norwegian Beamlines. The French authors also acknowledge the financial support of the ANR “NoMAC” (ANR-06-CO2-008). We also acknowledge helpful discussions with Professor A. M. Z. Slawin (University of St. Andrews).

**Supporting Information Available:** X-ray powder data on the as-prepared ScBDC, TGA data, N<sub>2</sub> adsorption isotherm and calorimetry at 77 K, and an adsorption isotherm and Langmuir plot for CH<sub>4</sub> on ScBDC at 230 K. Calorimetric heats of adsorption of methane are also reported. Crystallographic information files on all the crystal structures reported are deposited. This material is available free of charge via the Internet at <http://pubs.acs.org>.

LA803788U